ORIGINAL ARTICLE

Artemisia annua L. and photoresponse: from artemisinin accumulation, volatile profile and anatomical modifications to gene expression

Ellen M. Lopes[1] · Fábia Guimarães-Dias[2] · Thália do S. S. Gama[3] · Arthur L. Macedo[4,9] · Alessandra L. Valverde[4] · Marcela C. de Moraes[5] · Ana Cristina A. de Aguiar-Dias[6] · Humberto R. Bizzo[7] · Marcio Alves-Ferreira[2] · Eliana S. Tavares[8] · Andrea F. Macedo[1]

Abstract

Key message **Blue and yellow light affected metabolism and the morphology. Blue and red promote the DOXP/MEP pathway. *ADS* gene expression was increased in plants cultivated under blue, promoting artemisinin content.**

Abstract Artemisinin-based combination therapies are the most effective treatment for highly lethal malaria. Artemisinin is produced in small quantities in the glandular trichomes of *Artemisia annua* L. Our aim was to evaluate the effect of light quality in *A. annua* cultivated in vitro under different light qualities, considering anatomical and morphological changes, the volatile composition, artemisinin content and the expression of two key enzymes for artemisinin biosynthesis. Yellow light is related to the increase in the number of glandular trichomes and this seemed to positively affect the molecular diversity in *A. annua*. Yellow light-stimulated glandular trichome frequency without triggered area enhancement, whereas blue light stimulated both parameters. Blue light enhanced the thickness of the leaf epidermis. The B-promoting effect was due to increased cell size and not to increased cell numbers. Green and yellow light positively influenced the volatile diversity in the plantlets. Nevertheless, blue and red light seemed to promote the DOXP/MEP pathway, while red light stimulates MVA pathway. Amorpha-4,11-diene synthase gene expression was significantly increased in plants cultivated under blue light, and not red light, promoting artemisinin content. Our results showed that light quality, more specifically blue and yellow light, positively affected secondary metabolism and the morphology of plantlets. It seemed that steps prior to the last one in the artemisinin biosynthesis pathway could be strongly influenced by blue light. Our work provides an alternative method to increase the amount of artemisinin production in *A. annua* without the use of transgenic plants, by the employment of blue light.

Keywords *Artemisia annua* · Artemisinin · Glandular trichome · Light quality · Volatile

Abbreviations

ACT	Artemisinin combination therapies
ADS	Amorpha-4,11-diene synthase
B	Monochromatic blue light
CRY	Cryptochrome
CYP71AV1	Cytochrome P450 monooxygenase
D	Darkness
dNTPs	Deoxyribonucleoside 5′-triphosphate
DOXP/MEP	2*C*methyl-D-erythritol-4-phosphate pathway
DTT	Dithiothreitol
FAA	37% formaldehyde, glacial acetic acid, and 70% ethanol solution
G	Monochromatic green light
Gl.T	Glandular trichomes
LED	Light-emitting diode
LRI	Linear retention indices
MS	Murashige and Skoog
MVA	Mevalonic acid pathway

Communicated by Stefan Schillberg.

✉ Andrea F. Macedo
andrea.macedo@unirio.br; andreafm22@yahoo.com.br

Extended author information available on the last page of the article

NIST	National Institute of Standards and Technology
PAR	Photosynthetically active radiation
PDMS	Polydimethylsiloxane
PHOT	Phototropin
P.P	Palisade parenchyma
R	Monochromatic red light
SEM	Scanning electron microscopy
S.P	Spongy parenchyma
TT	T-shape trichome
W	White fluorescent light
Y	Monochromatic yellow light

Introduction

Artemisia annua L. is the only natural source of artemisinin, an expensive molecule with highly unstable supply on the market (Kazaz et al. 2016; Jolliffe and Gerogiorgis 2016; Ruan et al. 2016; Peplow 2018; Judd et al. 2019). Artemisinin is a sesquiterpene lactone with an endoperoxide group that is produced in small amounts solely in their glandular trichomes (Gl.T) (Ruan et al. 2016). Endoperoxides produced by plants are rare (Bilia et al. 2014). The total chemical synthesis or in vitro production of this molecule is complex and not yet economically advantageous (Xu et al. 2018). Artemisinin combination therapies (ACTs) are recommended by the World Health Organization (WHO) as the preferred treatment method for multidrug-resistant malaria (World Health Organization 2017). In 2015, approximately 429,000 deaths worldwide were caused by this illness, which affects poor and disadvantaged people (World Health Organization 2016). In addition to antimalarial activity, artemisinin and their derivatives have activity against cancer cells, schistosomiasis, and certain viral diseases, all of which are of great interest in human pharmacology (Ho et al. 2014).

In addition to artemisinin, the essential oil in *A. annua* is rich in monoterpenes, sesquiterpenes and phenols, and it represents another source of potential commercial value (Bhakuni et al. 2000). *Artemisia annua* essential oil can reach yields of 85 kg ha^{-1} (Bilia et al. 2014), and its extracts have been the focus of numerous studies demonstrating the antibacterial, antiviral, antioxidant, antifungal, analgesic, anti-inflammatory, herbicide and pesticide activities (Bhakuni et al. 2000; Brisibe et al. 2009; Melillo de Magalhães et al. 2012; Kim et al. 2015; Mesa et al. 2015; Ma et al. 2019).

Until now, only horticulture technologies have provided a better cost–benefit strategy to produce *A. annua* and its important metabolites (Milhous and Weina 2010; Kayser 2018). It is known that the content of essential oil and artemisinin is partially determined by genetic factors but also by abiotic factors (Tariq et al. 2014; Bryant et al. 2015). The increased demand for *A. annua* has mobilized intense research efforts to understand the dynamics of secondary metabolite production and plant growth (Liu et al. 2007). For example, the biochemical pathway of artemisinin is not yet clear, but there is evidence to suggest that the last step involves a non-enzymatic stage that requires only oxygen and light (Bryant et al. 2015; Ali et al. 2017).

Several sets of photoreceptors have been elucidated, which allow plants to respond to light. The model plant *Arabidopsis thaliana* has at least five phytochromes (red or far-red light receptors), two cryptochromes (Cry1 and Cry2) (blue light receptor), and two phototropins (Gonçalves et al. 2008). Only three papers concerning the effects of visible spectral light quality on *A. annua* have been published to date (Wang et al. 2001; Hong et al. 2009; Zhang et al. 2018) to elucidate how the quality of light changes the physiology of *A. annua*. However, none of those articles verified the influence of six different light quality treatments on the entire plantlet, concerning morphological and physiological aspects and therefore this area of study is completely new. Wang et al. (2001) determined that red light enhanced artemisinin content in hairy root cultures. Hong et al. (2009) suggested that overexpression of Arabidopsis CRY1 in *A. annua* resulted in increased accumulation of artemisinin. Recently, Zhang et al. (2018) evaluated the impact of far-red, white, blue, and red lights on artemisinin production. It has been recorded that blue and red light increased artemisinin and artemisinic acid content, that blue light led to amorpha-4,11-diene synthase (ADS) overexpression and that blue and red lights led to CYP71AV1 overexpression compared to controls (Zhang et al. 2018).

Assuming that secondary metabolite production can be influenced by light quality and that leaf morphology is mainly controlled by light (Galvão and Fankhauser 2015; Falcioni et al. 2017), we hypothesized that plantlets developed under standard in vitro culture conditions, with different radiation spectra, differ in metabolite quality and quantity, gene expression, trichome frequency and other leaf structural parameters. The glandular secretory trichomes present mainly in leaves have been considered an important resource of artemisinin, as well as other volatile metabolites (Nguyen et al. 2011; He et al. 2017). Previous studies have confirmed that ADS and cytochrome P450 monooxygenase (CYP71AV1), both key enzymes in artemisinin biosynthesis, are specifically expressed in the glandular secretory trichomes of young tissues (Liu et al. 2016; He et al. 2017). Therefore, we considered the morphological and molecular approaches to be vital to understanding how light quality can affect the trichome frequency, leaf area and tissues and volatile production. Our aim was to evaluate the effect of light quality in *A. annua* cultivated in vitro under different light qualities, considering anatomical and morphological

changes, the volatile composition and the expression of two key enzymes for artemisinin biosynthesis, *ADS* and *CYP71AV1*.

Materials and methods

Plant material and in vitro tissue culture

The seeds of *A. annua* from the genotype CPQBA-1 were provided by Dr. Pedro Melillo (UNICAMP/CPQBA). The seeds were cleaned and sown in sterile Murashige and Skoog (MS) growth medium (Murashige and Skoog 1962) supplemented with 30 g L^{-1} of sucrose and vitamins: 0.6 μM of myo-inositol; 2.43 μM of pyridoxine; 4.1 μM of nicotinic acid; 1.48 μM of thiamine, and solidified with 7 g L^{-1} of agar, pH adjusted to 5.7, without growth regulators (MS0). Two-month in vitro-grown plantlets were micropropagated in MS0, and light-quality experiments were performed in growth chambers (Controlled Environments) as described by Macedo et al. (2011). To provide different light qualities, plantlets were developed under white fluorescent light (W) (light-day, OSRAM®, 20 W) or under LED illumination (LHY, 110–112 V, 1 W, TASCHIBRA®) (approximately photosynthetically active radiation (PAR) = 10 μmol m^{-2} s^{-1}): monochromatic blue (B) (k_{max} = 475 nm), green (G) (510 nm), yellow (Y) (570 nm) and red (R) light (650 nm) (16 h of light and 25 °C), for 2 months as described (Fig. S1). Light-emitting diodes (LEDs) have been characterized by the wavelength specificity, relatively cool emitting surfaces, and linear photon output with an electrical input current (Mat Daud et al. 2016) W and darkness (D) conditions were used as control treatments to assess the effect of light on plantlets in the same medium formulation. PAR was measured using a PAR sensor coupled to an FMS2 Hansatech fluorometer (Hansatech, Instrument Ltd, King's Lynn, UK). A completely randomized design with 3 replications per treatment and 40 explants per replication was performed. Leaves from the third node of 2-month-old plantlets were harvested, starting from the apex, from plants grown under different wavelengths of the radiant spectrum or in the dark and subjected to the following analysis.

Leaf anatomy

Leaves were fixed in 37% formaldehyde, glacial acetic acid, and 70% ethanol solution (FAA) (Johansen 1940) and kept in 70% ethanol solution. Paradermal sections were created with a razor blade and stained with hydroalcoholic safranine (Johansen 1940). Cross-sections were obtained from the proximal, middle, and distal parts of the petiole and base, middle, and apex of the leaf blades. The samples were

embedded with Leica Historesin Embedding Kit and sectioned with a rotary microtome (American Optical). Sections were stained with toluidine blue (O'Brien et al. 1964).

For quantitative analyses, 30 leaves obtained from 30 different plants were used. Leaf area was measured using ImageJ® software (Wayne Rasband do Research Services Branch, National Institute of Mental Health, Bethesda, Maryland). Trichomes and the stomata frequency, as well as epidermis and mesophyll measurements, were obtained from five different portions of each leaf projected onto a 1 mm^2 graph paper with the support of a lucid chamber connected to a Zeiss AxiosKop 2, DEI-750 D, CE microscope supplied with a camera lucida. The photographs were obtained under an Olympus CH30 light microscope with an attached Olympus PM-C35B camera.

Histochemical tests

Leaves from 2-month-old grown plantlets from the different treatments were fixed in FAA for 24 h (Johansen 1940) and buffered neutral formalin (BNF) for 48 h. They were dehydrated through a tertiary butyl alcohol series (Johansen 1940), embedded in paraplast (Leica Microsystems Inc., Heidelberg, Germany) and then sectioned. The main classes of compounds were obtained using the following histochemical tests: Sudan black B and Sudan IV (Paerse 1980) for total lipids under visible light, respectively; Nile blue A (Cain 1947) for neutral and acidic lipids; ferric chloride (Johansen 1940) for phenolic compounds; vanillin–hydrochloric acid for tannins; Wagner's reagent (Furr and Mahlberg 1981) for alkaloids; ruthenium red (Gregory and Baas 1989) for acidic mucilage; tannic acid-ferric chloride for mucilage (Pizzolato and Larson 1977); and Lugol solution to detect starch (Pizzolato and Larson 1977). Standard control procedures were carried out simultaneously for all histochemical tests.

Electron microscopy

The leaf samples designated for scanning electron microscopy (SEM) analysis were fixed in 2.5% glutaraldehyde in 0.1 M phosphate buffer, pH 7.2, dehydrated in an ethanol series, and dried over the critical point (Peterson et al. 1978). The dried material was placed over aluminum stubs covered by a thin gold layer and examined using the SEM model LEO 1450 VP.

Sampling of volatiles by HS-SPME

Headspace solid-phase microextraction (HS-SPME) was used for volatile collection, followed by gas chromatography/mass spectrometry (GC/MS) determination (Reale et al. 2011). Leaf samples weighing 0.05 g obtained from four

different plantlets from each treatment were placed in a vial (5 mL) supplied with a Mininert valve (Supelco Inc., Bellefont, PA, USA) for HS-SPME analysis. For each plantlet treatment, the analysis was performed in triplicate. The vials were continuously heated in a plate (IKA-RH-KT/c) at 60 °C for 30 min to achieve the partition equilibration between the sample and the headspace. The polydimethylsiloxane (PDMS) 75 μm fiber (75 μm Carboxen™-PDMS StableFlex, Supelco) was then exposed to the headspace of the sample for 15 min at 60 °C to adsorb the analytes. The volatiles absorbed into the fiber were then thermally desorbed in the injection port of a GC at 250 °C for 3 min.

Gas chromatography/mass spectrometry

The analyses were performed in an Agilent 7890A gas chromatograph (Palo Alto, CA, USA) equipped with a flame ionization detector (GC-FID) and an Agilent HP-5MS (5% phenyl-methylpolysiloxane) fused silica capillary column (30 m × 0.25 mm, 0.25 μm). Hydrogen was used as the carrier gas at a flow rate of 1.0 mL min^{-1}. The oven temperature was programmed from 60 to 240 °C at 3 °C min^{-1}. The injector temperature was kept at 250 °C and the detector temperature at 280 °C.

Analyses by GC–MS were performed on an Agilent 5973N mass selective detector coupled to an Agilent 6890 gas chromatograph fitted with an HP-5MS fused silica capillary column (30 m × 0.25 mm, 0.25 μm). Helium was used as carrier gas at 1.0 mL min^{-1}. The mass detector was operated in electronic ionization mode (70 eV) at 3.15 scans s^{-1}, with a mass range from 40 to 450 μm. The transfer line was kept at 260 °C, with the ion source at 230 °C and analyzer at 150 °C. The oven temperature program and injection procedure were the same as above.

Identification of volatiles

The components were identified by comparison of their mass spectra with those from the Wiley Registry of Mass Spectral Data (McLafferty 2009) or National Institute of Standards and Technology (NIST) (Linstrom and Mallard 2016) databases, as well as by their linear retention indices (LRI), which were calculated according to van Den Dool and Kratz (1963), after injection of a homologous series of *n*-alkanes (C$_7$–C$_{26}$) under the same conditions described above, and compared with the literature data (Joulian and König 1998; Adams 2007).

Artemisinin content

Sixty-day-old plantlets without roots were dried in a ventilated oven (40 °C). Dried parts (40 mg) were extracted with 10 mL of ethanol using sonication (45 min). Extracts were evaporated and then solubilized in 1 mL of methanol. The procedure was performed in triplicate.

LC–MS experiments were performed using a Flexar SQ 300 LCMS system (PerkinElmer, Shelton, CT, USA) interfaced with a SQ 300 MS quadrupole mass spectrometer with electro-spray ionization as the ion source. The MS parameters were set at 12 L min^{-1} (300 °C) for the drying gas flow. Data acquisition was accomplished with Chromera software. LC analysis was performed using an analytical C18 column (PerkinElmer, 150 mm × 4.6 mm, 3 μm), and the mobile phase consisted of water (mobile phase A) and acetonitrile (mobile phase B), both with 0.1% formic acid, in a gradient starting with 55% B (9 min), which was increased to 100% B (1 min), maintained at 100% B (2 min), decreased to 55% B (1 min) and maintained at 55% B (2 min). The total run time per sample was 15 min. The flow rate was set at 1.2 mL min^{-1}, and the injection volume was 20 μL. A micro-splitter valve was used to send 45% of the flow to the mass spectrometer. The electrospray mass spectrometer (ESI–MS) was operated under positive ion mode. For quantitative analysis of artemisinin, SIM was used to record the abundance of the [M+H]$^+$ molecular ion peaks at *m/z* 283.1 for artemisinin. A calibration curve for quantification of artemisinin was obtained using five concentrations (1.5–80 μg mL^{-1}).

Total RNA isolation

The total RNA from leaf plantlet samples grown under different light qualities and in the dark was isolated using TRIzol® Reagent (Invitrogen) following the manufacturer's protocol. The RNA samples were treated with RNase-free DNase I (Biolabs) to eliminate DNA contamination. The RNA integrity was verified by electrophoresis on a 1% agarose gel, while the RNA concentration and purity were determined using a NanoDrop™ spectrophotometer ND-1000 (Thermo Scientific).

The expression levels of the *ADS* (amorpha-4,11-diene synthase; GenBank accession number JQ319661.1) and *CYP71AV1* (amorpha-4,11-diene 12-hydroxylase GenBank accession number DQ315671.1) (Wang et al. 2013) genes under the different treatments were evaluated by qPCR analysis. Primer pairs of 21–23 bp with a T_m of 60 °C ± 1 °C were designed with Primer3 plus software (Untergasser et al. 2007) and used to amplify a region of 80–200 bp of the target gene. To normalize the target gene expression under different treatments, the *ACT* gene served as a control (Actin, GenBank accession number EU531837) (Maes et al. 2011; Pu et al. 2013), which has been used previously in qPCR studies conducted in *A. annua*. The primer sequences and amplicon lengths are provided in Table S1.

The single strand of cDNA was synthesized by adding 1 µg of total RNA, 50 µM poly-dT (oligo dT20) and 10 µM each deoxyribonucleoside 5′-triphosphate (dNTPs). This mixture was incubated at 65 °C for 5 min and briefly chilled on ice. Then, 20 mM dithiothreitol (DTT), $1 \times$ First-Strand Buffer and 200 U reverse transcriptase SuperScript™ III (Invitrogen) were added to the mixture, and the total volume (20 µL) was incubated at 50 °C for 1 h following the manufacturer's instructions. The reverse transcriptase was inactivated by incubating the mixture at 70 °C for 15 min, and the solution was stored at − 20 °C. For each qPCR reaction, we added 10 µL of diluted cDNA (1:50), 0.2 µM of each primer, 50 µM of each dNTP, $1 \times$ PCR Buffer (Invitrogen), 3 mM of $MgCl_2$, 2 µL of SYBR® Green I (Molecular Probes) diluted in water (1:1000), and 0.25 units of Platinum Taq DNA polymerase (Invitrogen) in a total volume of 20 µL. The reaction mixtures were incubated for 5 min at 94 °C, followed by 40 amplification cycles of 15 s at 94 °C, 10 s at 60 °C (fluorescence measurement step) and 15 s at 72 °C. At the end of 40 cycles, a melting curve was generated (15 s at 95 °C, 15 s at 60 °C—fluorescence measurement step—and 15 s at 95 °C).

Polymerase chain reactions were performed using the 7500 Fast Real-time PCR detection system (Applied Biosystem) with SYBR® Green to monitor cDNA synthesis. The PCR efficiencies and optimal quantification cycle threshold or C_q value were estimated using Real-time PCR Miner software (Zhao and Fernald 2005). Three independent biological samples were evaluated using technical replicates. The relative expression level was calculated using the relative expression software tool (REST©).

Statistical analysis

The data were analyzed by one-way analysis of variance (ANOVA). The assumptions of ANOVA were fulfilled in all cases. The Tukey HSD test was used for multiple comparisons of the means. STATISTICA 7.0 software was used. The results are presented as the mean ± standard error (SE).

The relative expression level was calculated using the relative expression software tool (REST©). The REST tool compares two treatment groups with multiple data points in the sample versus control groups and calculates the relative expression ratio between them. The mathematical model that was used is based on the PCR efficiencies and the mean C_p deviation of target genes between the sample and the control group, normalized by the mean C_p deviation of the reference genes (Pfaffl 2001). In addition, the C_p values were analyzed by a Pair-wise Fixed Reallocation Randomization Test (Pfaffl 2001).

Results

Influence of light quality on plantlet morphology

The total leaf, blade and petiole area showed the same profile for all light treatments (Fig. 1a). The total leaf area was largest, followed by the leaf blade area and petiole area, in all light treatments when compared to D, in which the petiole area was larger than the leaf blade area (Fig. 1a). According to the Tukey test, light, independently of spectral quality, seemed to positively affect the total leaf area and leaf blade with respect to the dark control (Fig. 1a). The total leaf and blade area were significant higher in the positive control (W) (4.6 mm²) followed by B (3.7 mm²). Therefore, specific wavelengths and dark inhibited the area enhancement (leaf blade area and total leaf area). The petiole area was larger in plantlets grown under B (1.4 mm²) followed by W (1.1 mm²) and D (0.9 mm²) treatments (Fig. 1a). B seemed to trigger the increase in petiole area over other wavelengths.

In all light quality treatments, two types of trichomes were observed: glandular trichome (Gl.T) and non-glandular trichome (tector). The tector trichome was uniseriate, translucent, and composed of 4–5 cells, with a larger basal cell. The apex consisted of a bifurcated apical cell, giving the trichome the appearance of a T (T-shape) (T.T) (Fig. 2c). Gl.Ts were biseriate, translucent, and composed of a total of ten cells: two stalk cells, two basal cells, four subapical cells and two apical cells, which sometimes appeared much more turgid than the other cells (Fig. 2b–e). Light did not appear to affect the trichome structure, but it seemed to interfere with the stomata size, which was variable in plants grown in D, especially on the abaxial surface. The leaves were amphistomatic with anomocytic stomata in all treatments (Fig. 2).

Considering the total leaf blade area, the stomata frequency was statistically greater under W, in which we recorded the largest area (Fig. 1a, b). This result was significant when compared to the other treatments: B, followed by Y, R and finally G and D, in which the plantlets had the smallest total leaf blade area (Fig. 1b). The Gl.T frequency was higher and statistically similar in W, Y and B and less frequent in D. The T.T was more frequently observed in W followed by B and G and less in D, Y and R (Fig. 1b).

When comparing the frequency of Gl.T with T.T in the total leaf area, the results demonstrated no significant difference between the two types when the plantlets were cultivated under D (Fig. 1b).

Considering an area of only 300 µm² on the adaxial surface, the greatest number of stomata was recorded in plants grown under D and W; Gl.T occurred in greater frequency

Fig. 1 a Leaf area (μm²), **b** frequency of stomata and trichomes in the total leaf blade area (μm²) and **c** stomatal and trichome frequencies measured in five different areas of 300 μm² for each face of the leaf of *A. annua* plantlets cultured in MS0 under different light treatments and in the dark for 60 days. Mean ± SE ($n = 30$). Mean values with the same letter are not significantly different, based on ANOVA followed by Tukey's test at $p \leq 0.05$. (*) No significant difference between the quantification of the Gl.T and T.T under the different treatments
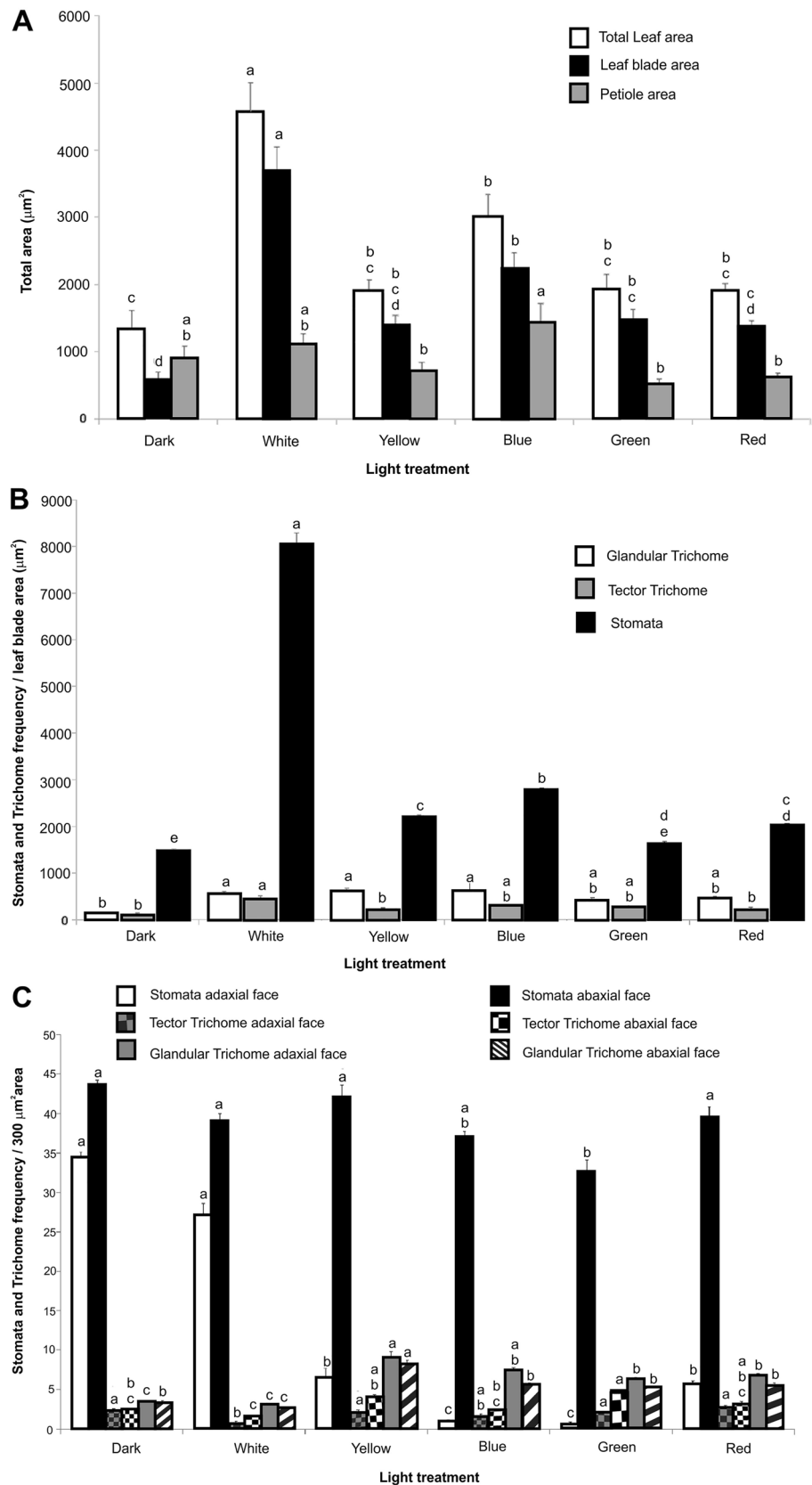
Fig. 2 MEV photos of *A. annua* trichomes. **a** The T-shape (T.T) trichome refers to light W; **b** glandular trichome (Gl.T) in D; **c** glandular trichomes under Y; **d** glandular trichome in B; **e** glandular trichomes in G; **f** glandular trichomes in R
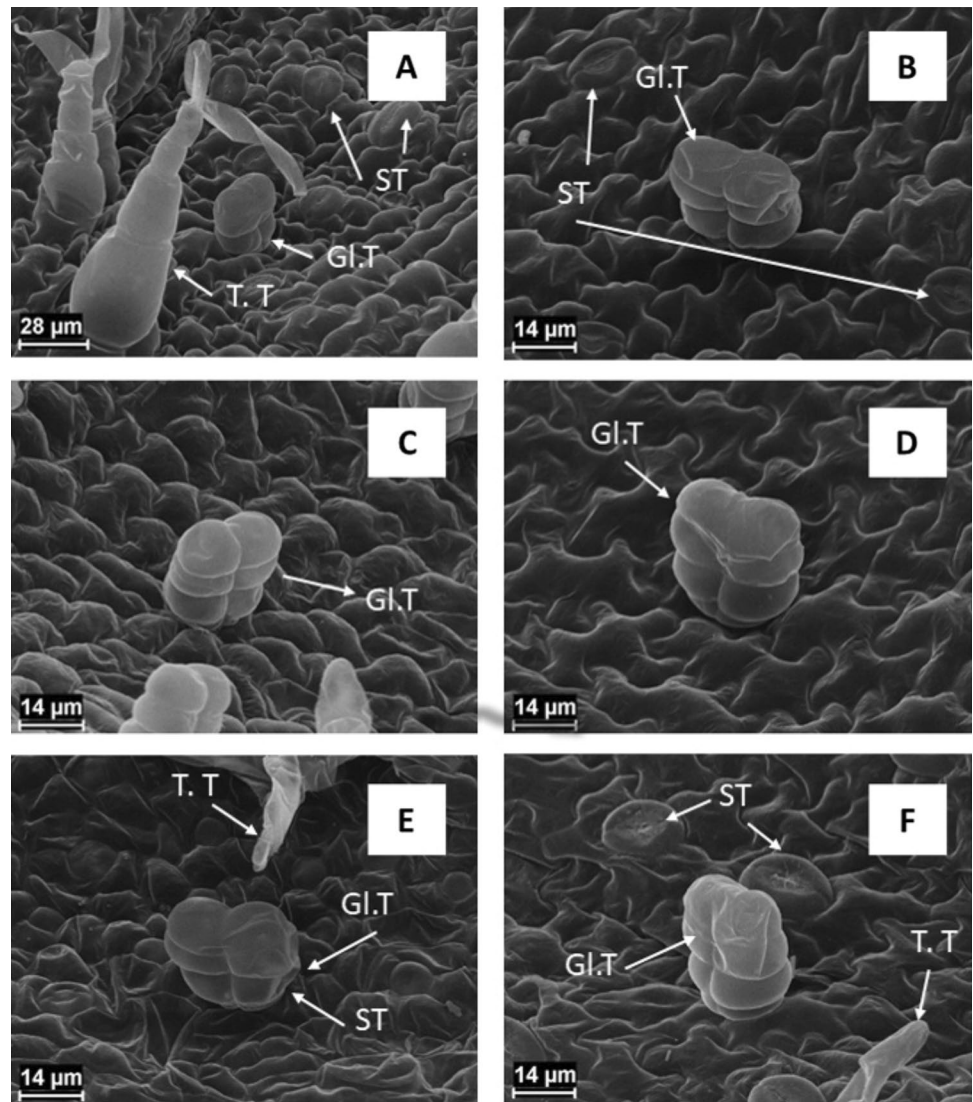
in Y, followed by B; the T.T frequency was higher in D, Y, G and R (Fig. 1c). The smallest amount of Gl.T was registered under W and D on the adaxial face (Fig. 1c). Therefore, on the adaxial surface, specific wavelengths inhibited the stomata frequency but stimulated the Gl.T frequency in *A. annua.*

The above result for Gl.T in 300 μm^2 was divergent from the results obtained for the total leaf area (Fig. 1a, c). When taking into consideration the number of Gl.T/total leaf blade area, the leaves grown in W, B and Y had the highest frequency without significant differences between them (Fig. 1b). In contrast, considering the amount of Gl.T/300 μm^2 on the adaxial face, the highest frequency was observed in Y, followed by B, G and R (Fig. 1c). The Gl.T frequency discrepancy between the total leaf blade area and in 300 μm^2 areas resulted from the leaf blade areas of leaves developed under B and W, which were the largest (Fig. 1a). Consequently, more Gl.T/total leaf blade area was expected

to be recorded in these treatments. However, the leaf blade area under Y light was statistically smaller compared with W and B.

On the abaxial surface, the greatest number of stomata was recorded in plants grown under D, Y, R and W (Fig. 1c). Gl.T was more abundant in Y and less in W, on both sides of the leaf, and T.T was more frequent in G (Fig. 1c). Y stimulated the Gl.T frequency without triggering area enhancement on both faces of the leaf. B stimulated both the Gl.T frequency and leaf blade area.

In general, the tissue thickness presented variations depending on the leaf region and treatment. Since the epidermis and parenchyma consisted of only one layer each, their thickness was directly correlated to the cell height (Figs. S2–S4, Tables S2–S4 and 1–3).

In the apical region of the leaf, the thickness of the epidermis was statistically greater under B on the abaxial surface and under B and R on the adaxial surface (Table 1). The

Table 1 Leaf parameters of the apex of the leaf blades of *L annua* L. plantlets cultured in MS0 under different light treatments and in the dark for 60 days

Light	Epidermis thickness (μm)[A]		Mesophyll thickness	Parenchyma thickness (μm)[C]	
	Adaxial face	Abaxial face		Spongy	Palisade
Dark	17.12 ± 0.01b	8.33 ± 0.24[B]c	30.06 ± 1.54d	Not observed	Not observed
White	17.25 ± 0.03ab	10.44 ± 0.57b	42.28 ± 1.17b	26.78 ± 1.10b	15.50 ± 0.59a
Yellow	17.23 ± 0.02ab	11.06 ± 0.52b	40.78 ± 2.94bc	26.61 ± 0.98b	11.17 ± 2.97b
Blue	17.38 ± 0.03a	12.72 ± 0.61a	50.00 ± 2.28a	39.33 ± 1.93a	11.78 ± 0.29b
Green	17.25 ± 0.02ab	13.11 ± 3.04bc	40.89 ± 1.51bc	26.56 ± 1.55b	14.33 ± 0.49a
Red	17.35 ± 0.11a	10.00 ± 0.39bc	35.12 ± 1.54cd	24.39 ± 1.40b	12.45 ± 0.41b

[A]Parameters measured of cross-section of the leaf blade: size of the thickness apex of the leaf blades

[B]Mean $\pm$ SE ($n = 30$)

[C]Mean values with the same letter are not significantly different, based on ANOVA followed by Tukey's test at $p \leq 0.05$

mesophyll and spongy parenchyma (S.P) thicknesses were greater in plantlets treated under B than the other treatments (Fig. S2F and Table 1). The palisade parenchyma (P.P) was thickest under D and G, in comparison to the other treatments (Fig. S2F and Table 1). However, mesophyll differentiation was less evident in D (Fig. S2F). The mesophyll under B was thicker due to the cellular height rather than the number of cellular layers (Table S2). The mesophyll was dorsiventral in all light treatments, except for leaves of plantlets grown under D, in which the mesophyll was homogeneous solely at the leaf apex (Fig. S2B). In the leaf apex, B stimulated many morphological parameters based on the enhancement of cell height in the epidermis and cell division in S.P. D had a negative effect, resulting in a reduced cell height.

In the middle third, the epidermis was thicker under B due to the enhancement of cell height, similar to the apex leaf area (Table 2 and Table S3). P.P. was thicker in W because of the increase in cell height (Table 2). The S.P. thickness showed the same results for all treatments; however, more layers were registered in D, which reduced the S.P. cell height (Table S3). The thickest mesophyll was observed in leaves treated under G due to the contribution

of the P.P since the S.P. thickness was statistically similar in all treatments (Table 2 and Fig. S3D). The number of mesophyll and S.P. cell layers was statistically greater in leaves under D; thus, S.P., D stimulated cell division and inhibited cell height (Table 2 and Fig. S3D). In the middle third, B and G stimulated many morphological parameters of cell height, but light inhibited cell division in S.P.

At the leaf base, no significant variation in the thickness of the epidermis was observed on the adaxial surface, but on the abaxial surface, the epidermal thickness was greater in D due to the contribution of the highest cell height in D (Fig. S4B, Tables 3, S4). The number of cell layers in the mesophyll was greater under D despite the absence of significant differences in thickness between treatments. Thus, cell height was likely inhibited in D compared with the other treatments (Tables 3, S4). The S.P. and P.P thickness were greater in W and smaller in B compared with all treatments (Tables 3, S4). As the number of P.P layers was the same for all treatments, the greater thickness of P.P. in W resulted from the contribution of cell height (Tables 3, S4). Light inhibited the epidermal thickness on the abaxial face and the number of cellular layers in the mesophyll, but it stimulated cell height.

Table 2 Leaf parameters of the middle third leaf blades of *Artemisia annua* L. plantlets cultured in MS0 under different light treatments and in the dark for 60 days

Light	Epidermis thickness (μm)[A]		Mesophyll thickness	Parenchyma thickness (μm)[C]	
	Adaxial face	Abaxial face		Spongy	Palisade
Dark	11.39 ± 0.38[B]b	81.89 ± 0.51ab	42.72 ± 1.51b	27.06 ± 1.31a	16.00 ± 0.57bc
White	9.11 ± 0.44c	10.06 ± 0.42c	46.22 ± 1.49ab	27.50 ± 1.01a	18.72 ± 0.90a
Yellow	10.56 ± 0.43bc	10.06 ± 0.41c	43.85 ± 1.12b	29.33 ± 0.93a	14.50 ± 0.43cd
Blue	14.17 ± 0.75a	12.78 ± 0.54a	40.05 ± 2.20b	27.22 ± 2.27a	13.11 ± 0.64d
Green	9.94 ± 0.50bc	11.28 ± 0.44abc	61.17 ± 8.71a	28.22 ± 1.32a	16.94 ± 0.33ab
Red	10.17 ± 0.32bc	10.33 ± 0.34bc	44.11 ± 3.02b	28.56 ± 1.02a	12.56 ± 0.41d

[A]Parameters measured in a cross-section of the leaf blade: size of the thickness apex of the leaf blades

[B]Mean $\pm$ SE ($n = 30$)

[C]Mean values with the same letter are not significantly different, based on ANOVA followed by Tukey's test at $p \leq 0.05$

Table 3 Leaf parameters of the base leaf blades of *Artemisia annua* L. plantlets cultured in MS0 under different light treatments and in the dark for 60 days

Light	Epidermis thickness (µm)[A]		Mesophyll thickness	Parenchyma thickness (µm)[C]	
	Adaxial face	Abaxial facet		Spongy	Palisade
Dark	10.78 ± 0.39[B]a	12.61 ± 0.41a	46.67 ± 1.60a	31.61 ± 1.14ab	16.06 ± 0.53b
White	12.06 ± 0.74a	12.22 ± 0.46ab	50.94 ± 2.11a	34.17 ± 1.95a	18.11 ± 0.78a
Yellow	9.33 ± 0.34a	10.17 ± 0.40c	38.56 ± 1.28a	27.50 ± 1.21bc	12.06 ± 0.37c
Blue	10.89 ± 0.48a	11.61 ± 0.60abc	36.61 ± 1.76a	24.39 ± 1.71c	12.22 ± 0.53c
Green	10.56 ± 0.42a	10.06 ± 0.28c	53.17 ± 1.70a	28.50 ± 1.48bc	16.17 ± 0.51b
Red	12.35 ± 0.30a	10.67 ± 0.43bc	45.86 ± 1.46a	28.97 ± 1.64abc	14.89 ± 0.37b

[A]Parameters measured in a cross-section of the leaf blade: size of the thickness apex of the leaf blades

[B]Mean $\pm$ SE ($n = 30$)

[C]Mean values with the same letter are not significantly different, based on ANOVA followed by Tukey's test at $p \leq 0.05$

Influence of light quality on leaf histochemistry

The Abraham-modified reaction revealed sesquiterpene lactones in response to the W, Y, B and R treatments in Gl.T (Table 4). Y, B and G had the same metabolic class profile with respect to total and neutral lipids and phenolic compounds (Table 4). Positive results were obtained for total lipids in the G, Y and B treatments (Fig. S5D). For neutral lipids and alkaloids, positive results were only obtained in plantlets treated under Y (Fig. S5F). Acidic mucilage and alkaloids were detected in W and Y (Table 4). The presence of starch in the trichomes was unique to the control treatments (W and D). Plantlets developed under Y showed a great diversity of chemical classes when compared to the other treatments. In contrast, plants that were developed under D and R had fewer chemical classes than those grown under different bands of the radiation spectrum (Table 4 and Fig. S5).

Influence of light quality on leaf volatile profile

Forty-six volatile compounds were identified. Among the plant volatiles associated with the different treatments,

sesquiterpenes predominate (25). The results revealed quantitative and qualitative molecule variation between the different treatments. The greatest compound diversity was identified in G, and the lowest was observed in B and R (Table 5). The mixture of *p*-cymene, limonene and 1,8-cineole (W); myrcene (D) and camphor (W) were the relative most abundant. Other minor constituents were 4-(*E*)-octene, α-thujene, *trans*-β-ocimene, 3-hexenyl 2-methylbutanoate, 2-modhephene, β-acoradiene, *trans*-calamene, (*E*)-γ-bisabolene, α-*cis*-bergamotene. 4-(*E*)-octene and carvone occur solely in W (Table 5). More monoterpenes were detected in W and sesquiterpenes in G than in the other treatments (Table 5). Esters were more diverse in G and less common in B and D (Table 5).

Influence of light quality on artemisinin content

All treated groups produced less artemisinin than W ($p < 0.0001$) and more than D ($p < 0.0001$) (Fig. 3a). White light, the positive control, induced a greater accumulation of artemisinin, as expected since white light is composed of all wavelengths of the light spectrum (Fig. 3a). Among the treated groups, the plantlets grown in Y and in G did not

Table 4 Summary of the results obtained in the histochemical characterization of glandular trichomes in leaves of *Artemisia annua* L.

Histochemical tests	Identified classes of compounds	White	Dark	Yellow	Blue	Green	Red
Sudan black B	Acid lipids	–	–	+	+	+	–
Sudan IV	Total lipids	–	–	+	+	+	–
Nile blue A	Neutral lipids	–	–	+	+	+	–
Ferric chloride	Phenolic compounds	–	–	+	+	+	–
Vanillin-hydro chloric acid	Tannins	–	–	–	–	–	–
Wagner's reagent	Alkaloids	–	–	+	–	–	–
Ruthenium red	Acidic mucilage	+	–	–	–	–	–
Tannic acid and ferric chloride	Mucilage	–	–	–	–	–	–
Lugol	Starch	+	+	–	–	–	–
Abraham modified reaction	Sesquiterpene lactone	+	–	+	+	–	+

(+) positive results, (−) negative results

Table 5 Leaf volatile constituents from 60-day-old *Artemisia annua* L. plantlets cultivated in vitro under different light treatments

Identification	RI[a]	RI[b]	Dark	White	Yellow	Blue	Green	Red
4-(*E*)-Octene (H)[c]	802	801[d]	–	0.2	–	–	–	–
Ethyl 2-methylbutanoate (*E*)	849	850	1.2	1.8	0.8	1.1	1.2	1.9
α-Thujene (M)	925	924	–	0.2	0.1	–	–	0.5
α-Pinene (M)	930	932	0.8	0.2	0.6	1.5	1.1	0.6
Camphene (M)	944	946	1.1	2.1	1.5	2.6	1.5	4
Sabinene (M)	957	969	–	0.9	0.8	–	0.5	1.7
Myrcene (M)	1000	988	47.3	17.9	43.7	27.9	35.7	10.4
α-Phellandrene (M)	1006	1002	2.7	1	–	3.8	3.2	1.8
α-Terpineol (M)	1016	1014	0.5	0.4	0.4	0.6	–	0.5
p-Cymene + limonene (M) + 1,8-cineole (M)	1030	1029	6.6	30.5	8.9	18.7	12.5	18.4
Butyl 2-methylbutanoate (*E*)	1041	1047	–	–	0.2	–	0.4	–
trans-β-Ocimene (M)	1051	1044	0.2	0.1	0.3	0.4	0.3	–
Artemisia alcohol (M)	1062	1080	2.4	0.6	4.2	6.9	2.8	–
2-Methyl butyl isovalerate (*E*)	1110	1103	0.5	1.7	1.3	6	1	2.3
allo-Ocimene (M)	1134	1128	–	0.4	–	0.4	0.2	0.5
Camphor (M)	1149	1141	2.9	17.9	6	6.7	5.5	14.8
Octyl acetate (NT-A)	1163	1197	–	0.7	–	–	0.3	1.1
cis-Sabinene acetate (M)	1226	1219	–	0.4	0.5	–	0.3	–
3-Hexenyl 2-methyl butanoate (P)	1237	1090	–	0.5	0.1	–	0.2	–
cis-3-Hexenyl isovalerate (*E*)	1240	1241	0.3	0.3	0.3	–	0.2	–
Carvone (M)	1245	1239	–	0.3	–	–	–	–
α-Cubebene (S)	1348	1345	0.2	0.2	0.2	–	0.3	0.4
α-Copaene (S)	1377	1374	1.5	–	0.3	0.2	0.7	–
2-Modhephene (S)	1384	1382	–	0.1	–	–	0.2	–
Identification	RI[a]	RI[b]	Dark	White	Yellow	Blue	Green	Red
Hexyl hexanoate (*E*) + β-elemene (S)	1392	1389	1.1	1.9	1.6	0.9	1.2	2.2
β-Isocomene (S)	1400	1407	0.5	–	–	–	0.4	–
cis-Caryophyllene (S)	1406	1408	0.5	–	0.2	0.2	0.3	0.6
α-*cis*-Bergamotene (S)	1411	1411	0.2	–	–	–	0.2	–
trans-β-Caryophyllene (S)	1417	1416	1.3	1.5	0.6	0.6	1	4.5
β-Copaene (S)	1430	1430	0.8	–	0.3	0.5	0.6	0.7
γ-Elemene (S)	1435	1434	–	0.2	–	–	0.2	0.5
E-β-Farnesene (S)	1463	1454	9.7	0.8	4.3	2.1	6.1	3.7
β-Acoradiene (S)	1470	1469	1.1	0.1	0.2	0.3	0.6	0.5
β-Chamigrene (S)	1479	1476	4.2	2.5	6.2	3.4	3.6	2
ar-Curcumene (S)	1485	1479	2.5	2.2	1.6	1.2	2.2	0.5
α-Selinene (S)	1495	1498	1.2	1	1.1	0.5	0.9	1.1
epi-Zonarene (S)	1499	1501	0.6	0.3	0.2	0.3	–	1.1
β-Bisabolene (S)	1510	1505	–	0.4	0.8	–	0.3	1.1
Isobornyl isovalerate (S)	1517	1521	–	–	0.5	–	0.6	–
7-*epi*-α-Selinene (S)	1524	1520	1	0.6	0.5	0.6	0.6	2.6
trans-Calamenene (S)	1531	1521	–	–	0.2	–	0.2	–
(*E*)-γ-Bisabolene (S)	1537	1529	0.1	0.1	0.2	0.2	0.2	0.4
cis-Calamenene (S)	1542	1528	–	–	–	0.4	0.4	–
Caryophyllene oxide (S)	1576	1582	0.4	0.5	0.9	0.4	0.7	0.6
Intermedeol (S)	1666	1665	0.4	–	–	–	0.6	–
Total			93.8	90.5	89.6	88.4	89	81
Number of metabolites identified			30	35	34	27	40	29

[a]Linear retention indices in a DB-5 column

[b]Reference retention indices. Literature reference: Adams (2007)

[c]*E* ester, *NT-A* non-terpene alcohol, *S* sesquiterpene, *M* monoterpene, *H* hydrocarbon

[d]From the NIST database (Linstrom and Mallard 2016)
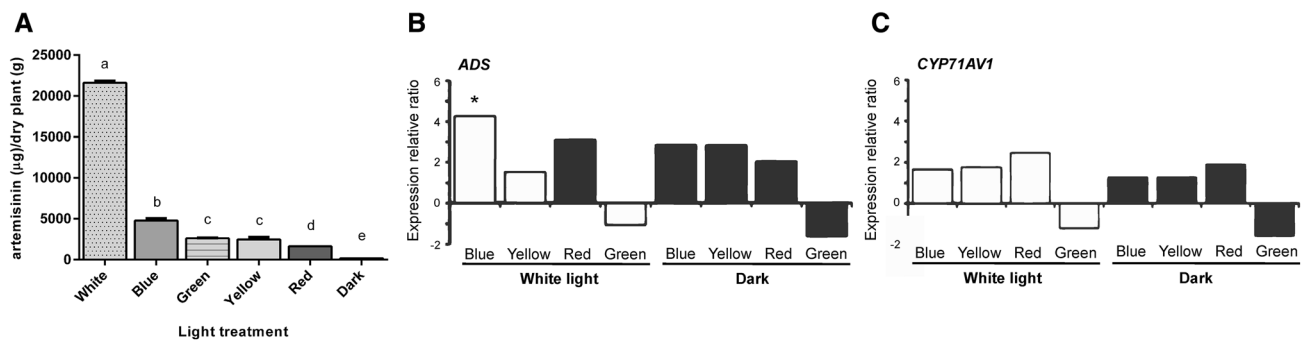
Fig. 3 a Artemisinin content (µg) per gram of dry aerial parts for each light treatment ($p \leq 0.05$) and relative expression ratio of *ADS* and *CYP71AV1* genes in *A. annua* leaves under different light regimes. **b** *ADS*, **c** *CYP71AV1*. The reference gene Actin was used to normalize the qPCR data. The relative expression level was cal-

culated using the relative expression software tool (REST©), and the C_p values were analyzed using a Pair-Wise Fixed Reallocation Randomization Test. *Indicates significant differences in gene expression between color light treatment and the control treatments (plant grown under white light and in the dark)

show a significant difference ($p = 0.9130$) (Fig. 3a). Plantlets grown in B showed increased production of artemisinin ($p < 0.0001$), and those grown in R showed reduced production ($p < 0.0006$) (Fig. 3a).

Influence of light quality on ADS and CYP gene expression

The *ADS* and *CYP71AV1* genes showed distinct expression profiles under different light treatments. *ADS* gene expression was significantly upregulated (Fig. 3b) in plantlets grown under B compared with plantlets grown under the positive control condition (W). No significant differences in *ADS* expression were observed between the light treatments Y, R and G when compared to the positive control condition. In addition, no differences in *ADS* gene expression were observed between W and D (Fig. 3b). Expression of the *CYP71AV1* gene was also accessed by qPCR under the above-described light treatments, and no significant differences were observed (Fig. 3c).

Discussion

Light perception and regulation are controlled by a network of photoreceptors such as phytochromes (red/far-red receptors, 680–735 nm), cryptochromes (blue/UV-A light receptors, 340–520 nm), and phototropins (Folta and Carvalho 2015). To investigate the effect of light quality on responses in *A. annua,* we used the light-emitting diode (LED) technology, which provides the best opportunity because it allows precise control over irradiance- and spectrum-induced plant responses and the adjustment of light output from individual light sources (Pashkovskiy et al. 2016).

The present investigation in *A. annua* is very relevant for the following reasons: (a) there is a high global demand

for the plant and its metabolites; (b) there is an urgent need to optimize at least artemisinin synthesis; and (c) there is a lack of knowledge about the effect of light on this species. Different LED light and D inhibited the total leaf area, leaf blade area, stomata and T.T frequency compared with W in in vitro-developed *A. annua* plantlets (Figs. 1b, S1). Light, independent of wavelength seemed to be an important factor for T.T or Gl.T, inducing mesophyll differentiation mainly in the middle third and artemisinin production in *A. annua* (Fig. 2, Figs. S2B, S3B and S4B). In addition, some of the studied parameters were positively affected by D, such as cellular division in the mesophyll, middle third and leaf base (Tables 2, 3, Figs. S2B and S3B).

In general, among specific types of spectral light, B enhanced, and R inhibited morphological features. B enhanced thickness of the epidermis in the leaf apex and in the middle third on both leaf faces, mesophyll and S.P thickness in the middle third; and cell division in S.P in the leaf apex (Fig. 1a, Tables 1, 2). According to many authors, B induces and R prevents increases in leaf thickness (Li et al. 2010; Macedo et al. 2011; Liu et al. 2014). The B-promoting effect was due, mainly, to increased cell size and not to increased cell numbers. In the leaf blade, B seemed to promote size enhancement in different directions (Macedo et al. 2011; Fan et al. 2013). This result was also observed by Fukuda et al. (2008). This reaction reflects the observations on pepper (Schuerger et al. 1997), wheat (Goins et al. 1997) and *Ficus benjamina* (Zheng and Van Labeke 2017) where increased levels of B to R increased the leaf area, epidermal cells, palisade and spongy mesophyll thickness. In *Platycodon grandiflorum*, B induced increased leaf thickness than R (Liu et al. 2014). Similarly, leaf thickness was higher in cotton (*Gossypium hirsutum* L.) grown with R and B LEDs compared to 100% R LEDs (Li et al. 2010). Some authors have reported that the light quality can interfere with the thickness (Gonçalves et al. 2008), the differentiation of the

mesophyll, cell division, and development of the leaf (Liu et al. 2014).

Concerned to differentiation, it was clearly observed in the present work that the light quality interfered in tissue differentiation. Seedlings developed in Y and G presented the single-layered palisade tissue with less elongated cells than in W, R and B (Fig. S2). Specifically in D most of the cells were rounded (Fig. S2B). Therefore, cell elongation in the tissue layers appears to be a continuous phenomenon, depending on the interaction with the light spectrum composition, where B is relevant for *A. annua* (Izzo et al. 2019). A typical dorsiventral leaf anatomy (with two clearly distinct tissues and functions) can be interpreted as a plastic adaptation of the mesophyll structure to light quality (Izzo et al. 2019).

Some of the studied parameters were positively affected by a specific wavelength spectrum compared with both controls and the other light qualities tested, including Y and G, both of which have remained poorly studied. Y, G and B affected important aspects of *A. annua*, which were correlated to the biosynthesis of relevant metabolites and to the increase in size of metabolite production sites. B has been better studied than Y and G. B receptors: cryptochromes (CRY1-3) and phototropins (PHOT1 and 2) have been found in many plant species (Folta et al. 2003; Wu et al. 2013; Hayes et al. 2014). In the present work, were used low light intensities, which have been correlated to CRY2 responses (Demarsy and Fankhauser 2009). The importance of G and Y absorption remains to be fully understood, and knowledge gaps persist regarding the influence of the light spectrum on plant metabolism, growth and morphology (Bergstrand et al. 2015).

Previous studies have demonstrated that artemisinin biosynthesis and essential oil production are localized mainly in leaf Gl.T in *A. annua.* The trichome frequency could be a key factor for the improvement of artemisinin content and other metabolites (Lommen et al. 2006; Yadav et al. 2014; Tan et al. 2015). Many key genes in terpenoid biosynthesis are mainly expressed in trichomes (Wang et al. 2002; Ennajdaoui et al. 2010; Sultana et al. 2015). Therefore, a higher frequency of trichomes can increase the production of artemisinin and other metabolites in the plants (Xiao et al. 2016). According to Xiao et al. (2016), the modification of certain aspects of leaf morphology, such as the trichome frequency, could be an alternative to optimize the yield of volatiles and artemisinin. In the present study, Y increased the Gl.T frequency without triggering area enhancement (Fig. 1a, b). In contrast, B stimulated both parameters (Fig. 1a, b). It is well known that trichome number and size are partly regulated by light (Booth et al. 2017). Yu et al. (2017) reported that leaf area of plants was greatest for seedling grown under R, and lowest under B. In the present study, B also seemed to enhance petiole area and stomatal frequency/total leaf area

(Fig. 1a, b). It is well known that stomatal development is light dependent (Klermund et al. 2016). In accordance with our results, B LED light increases the number of stomata in *Vitis vinifera* (Poudel et al. 2008). On the other hand, Yu et al. (2017) reported that B reduced the stomata number per unit area more than R and Y in *Camptotheca acuminata*. However, many authors have reported that light quality effects on plant growth, flowering time, and the contents of secondary metabolites are species-specific (Massa et al. 2008; Singh et al. 2015).

The biosynthesis of compounds in plants, such as phenolics, terpenoids, alkaloids, and others secondary metabolites, can also be induced by light quality (Fiutak et al. 2019). Light, in terms of quality and quantity, is one of the most important environmental factors affecting the synthesis of these compounds (Wang et al. 2007). The biosynthesis of phenolic compounds, for example, requires light or is enhanced by light (Ghasemzadeh and Ghasemzadeh 2011). Previous studies have demonstrated that different light intensities and qualities promoted an increase in the production of phenolic compounds in medicinal plants (Karimi et al. 2013). According to histochemical tests, Y induced the production of more chemical classes, followed by B and G, and R had a negative effect (Table 4). Y, B and G were related to phenolic compound detection and Y and B to sesquiterpene lactones (Table 4). According to Tariq et al. (2014), who studied the influence of different light qualities on calluses of *A. absinthium,* G, B and Y stimulated total phenolic contents compared with R, W and D. Cultures of *Swertia chirata* exposed to B exhibited the maximum accumulation of polyphenols (Dutta Gupta and Karmakar 2017). Y and B treatments promote starch accumulation in *Oncidium* plantlets (Li et al. 2010). In our results, only leaves cultivated under D and W accumulated starch. Under W treatment, photosynthesis could occur more effectively, and therefore the plant reserved the starch (Johkan et al. 2012). In D, photosynthesis did not occur, although according to Biesboer and Mahlberg (1978), plantlets reserved and synthesized starch in D due to the presence of exogenous sugars.

Artemisia annua volatiles show great variability in terms of their quantitative and qualitative composition (Tzenkova et al. 2010; Bilia et al. 2014; Coşge Şenkal et al. 2015), which depend on geographic origin, season, analyzed plant part, soil, extraction method, chemotype, choice and stage of drying conditions (Omer 2013; Zhigzhitzhapova et al. 2019). Some terpenes, such as α-thujene (0.5 in R), α-pinene (1.5 in B), camphene (4.0 in R), sabinene (1.7 in R), phellandrene (3.8 in B), limonene, 1,8-cineole, artemisia alcohol (6.9 in B), camphor (17.9 in W), α-terpineol (0.6 in B), α-copaene (1.5 in D), β-elemene (0.5 in R), *trans*-caryophyllene (0.6 in R), *trans*-β-farnesene (9.7 in D), and selinene (1.2 in D), were detected in our in vitro-developed plantlets (Table 5) and have being identified in *A. annua* essential oil (Ruan

et al. 2016). *Artemisia annua* is rich in terpenoids, with 134 monoterpenes and 174 sesquiterpenes (Brown 2010; Xie et al. 2016). Farnesene, caryophyllene, and 8-epi-cebrol are prevalent sesquiterpenoids in *A. annua*. Linalool, camphor, and 1,8-cineole are also common terpenoids (Xie et al. 2016). The large number of terpenoids indicates the complexity of a biosynthetic network in this anti-malarial plant (Xie et al. 2016). These compounds have important commercial and ecological significance, and their presence in plants is usually induced by the light conditions (Wu et al. 2013). However, previous work has shown that high light intensity decreased sesquiterpenes in plantlets (Alvarenga et al. 2015). Some detected compounds, including the major ones like myrcene (47.3 in D, 43.7 in Y), camphor (17.9 in W), *p*-cymeno, 1,8-cineole, limonene (30.5 in W), α-phellandrene (3.8 in B), artemisia alcohol (6.9 in B), and α-pinene (1.5 in B) (Table 5), have been noted not only to antibacterial and antifungal activity but also for their utility in the aroma industry (Perazzo et al. 2003; Ali et al. 2017) (Table 5).

G followed by Y seemed to positively influence the diversity of the molecules detected in the in vitro-developed *A. annua* aroma (Table 5). The least complex profile was observed in plants grown under B and R totaling 27 and 29 chemical constituents detected, respectively (Table 5). The lowest total content of metabolites was observed in plantlets grown under B and R (Table 5). On the other hand, most sesquiterpenes had greater relative abundance in R and most monoterpenes were more strongly expressed in B followed by R compared to all treatments (Table 5).

Two separate biosynthetic pathways, the cytosolic mevalonic acid (MVA) and the plastidic 2*C*methyl-D-erythritol-4-phosphate (DOXP/MEP) pathways, are involved in plant terpene biosynthesis (Mahmoud and Croteau 2002). Monoterpenoids come from the DOXP/MEP pathway and occur in plastids (Mahmoud and Croteau 2002). Sesquiterpenoids come from MVA, which occurs in cytosol (Mahmoud and Croteau 2002). According to the present study, B and R seemed to promote the DOXP/MEP pathway, while R stimulate MVA pathway. The effects of B can be perceived by blue light-specific photoreceptors as cryptochromes, but also by the phytochrome system (Ahmad and Cashmore 1997). In addition, recent work has shown that cryptochromes and phytochromes share some common signaling pathways (Mishra and Khurana 2017). In the present work, both phytochrome and B-specific photoreceptors could be involved in the accumulation of mono- and sesquiterpenes in *A. annua*. The intermediates from MEP/DOXP and MVA were exchangeable, for that reason R seemed to stimulate both pathways (Inthima et al. 2017). These results are in agreement with the work of Ren et al. (2014) that also observed reduction of terpenes under R. Lazzarini et al. (2018) also observed a reduction in the number of molecules detected

under B. On the other hand, B has been shown to induce greater biosynthesis of α-pinene in tomato leaf (Arena et al. 2016), and similar results were observed herein (Table 5). Among the specific wavelengths, B increased the relative content of *p*-cymene + limonene + 1,8-cineole in *A. annua* leaves (Table 5). A positive effect on 1,8-cineole content has been observed in peppermint cultivated under B (Maffei and Scannerini 1999). Limonene concentrations, according to Kong et al. (2006), are higher in leaves of *Perilla* plantlets treated with B. Studies in *Mikania glomerata* Spreng., *Ocimum gratissimum* L., *Melissa officinalis* L. and *Piper aduncum* L. showed similar results, with high essential oil contents when grown under low light intensities and enriched environments with B (Pacheco et al. 2016). Alvarenga et al. (2015) observed enhancement of the monoterpene sabinene under R.

Gene expression analysis of the genes encoding key enzymes in artemisinin biosynthesis showed that *ADS* gene expression was significantly increased in plants cultivated under B (Fig. 3b, c). We also showed that the level of artemisinin was higher in plants cultivated under B (Fig. 3a). In *A. thaliana*, two cryptochromes (CRY1 and CRY2) enable it to respond to B (Briggs and Olney 2001). In addition, Hong et al. (2009) showed that overexpression of *A. thaliana CRY1* in *A. annua* increased the transcript abundance of the *ADS* gene (Hong et al. 2009; Han et al. 2014; Bryant et al. 2015; He et al. 2017). Zhang et al. (2018) concluded that red and blue light enhanced the artemisinin content and the expression of amorpha-4,11-diene synthase (ADS) and cytochrome P450 monooxygenase (CYP71AV1) genes. These results partially corroborate our observations. In the present work, R is not involved in artemisinin accumulation, neither CYP71AV1 gene expression compared to the controls. We suggest that CRY2 is involved in the induction of *ADS* gene expression in response to B, promoting artemisinin content. Several studies have suggested that *ADS* is a key enzyme in artemisinin biosynthesis (Han et al. 2014; Shi et al. 2017). Transgenic plants carrying RNAi constructs targeting the *ADS* gene show decreased contents of artemisinin, artemisinic acid, and arteannuin (Ma et al. 2015). In addition, artemisinin levels are significantly enhanced in transgenic lines over-expressing the *ADS* gene (Ma et al. 2015). Shi et al. (2017) overexpressed *ADS* in combination with three other enzymes in the artemisinin biosynthetic pathway in *A. annua* to successfully promote artemisinin production. These studies definitively link artemisinin production to the presence of B as well as the expression of *ADS*. Our work is partially consistent with previous studies.

In conclusion, the results from the present study confirmed our hypothesis that different radiation spectra affect morphological aspects, gene expression, quality and quantity of metabolites in different ways. Our results showed that light quality, more specifically B and Y, positively

affected secondary metabolism and the morphology of plantlets. Our results, through histochemical assays, volatile analysis and frequency of glandular trichomes, showed that Y is related to the increase in the number of glandular trichomes and this seemed to positively affect the molecular diversity in *A. annua*. These results are in disagreement with previous works where Y seemed to be deleterious for several parameters in plants (Wu et al. 2014; Su et al. 2013; Liu et al. 2018). B affected many anatomical aspects, especially those related to the leaf and petiole area, trichome frequency, epidermis and mesophyll differentiation and thickness. R and B affected the mono- and sesquiterpenes relative abundance. Analysis of gene expression suggested that only the *ADS* gene was induced by B and it enhanced artemisinin content. It seemed that steps prior to the last one in the artemisinin biosynthesis pathway could be strongly influenced by B. Previous studies have demonstrated that the promotion of *ADS* expression by B may be directly responsible for the increase in artemisinin production. Therefore, our work provides an alternative method to increase the amount of artemisinin production in *A. annua* without the use of transgenic plants, by the employment of blue light. Regarding the histochemical, anatomical and volatile results presented in this study, the effects of yellow and green light on plant physiology merit more attention.

Author contribution statement AFM supervised the project; AFM, EST, MA-F, HRB, ACAA-D and ALV designed the experiments; EML, EST and AFM wrote the manuscript, with the participation of FG-D, ALM and contributions from all authors; tissue culture experiments were conducted by EML and AFM; morphological assays were conducted by AFM, EST, TSSG and ACAA-D; volatile assays were advised by HRB and conducted by EML and AFM; artemisinin analysis was conducted by ALM under the supervision of ALV and MCM; gene expression assays were conducted by EML and FG-D under the supervision of MA-F. All authors critically revised the manuscript and gave their final approval.

Data availability statement The data that support the findings of this study are available from the corresponding author upon reasonable request.

Compliance with ethical standards

Conflict of interest There is no conflict of interest.

References

Adams RP (2007) Identification of essential oil components by gas chromatography/mass spectrometry, vol 456. Allured Publishing Corporation, Carol Stream

Ahmad M, Cashmore AR (1997) The blue-light receptor cryptochrome 1 shows functional dependence on phytochrome A or phytochrome B in *Arabidopsis thaliana*. Plant J 11:421–427

Ali M, Abbasi BH, Ahmad N, Khan H, Ali GS (2017) Strategies to enhance biologically active-secondary metabolites in cell cultures of *Artemisia*—current trends. Crit Rev Biotechnol 37(7):833–851

Alvarenga ICA, Pacheco FV, Silva ST, Bertolucci SKV, Pinto JEBP (2015) In vitro culture of *Achillea millefolium* L.: quality and intensity of light on growth and production of volatiles. Plant Cell Tissue Organ Cult 122(2):299–308

Arena C, Tsonev T, Doneva D, De Micco V, Michelozzi M, Brunetti C, Centritto M, Fineschi S, Velikova V, Loreto F (2016) The effect of light quality on growth, photosynthesis, leaf anatomy and volatile isoprenoids of a monoterpene-emitting herbaceous species (*Solanum lycopersicum* L.) and an isoprene-emitting tree (*Platanus orientalis* L.). Environ Exp Bot 130:122–132

Bergstrand KJ, Asp H, Schüssler HK (2015) Different light spectra is affecting growth and morphology of transplants of *Solanum lycopersicum*. In: International symposium on new technologies and management for greenhouses-GreenSys2015 1170:937–942

Bhakuni RS, Jain DC, Sharma RP, Kumar S (2000) Secondary metabolites of *Artemisia annua* and their biological activity. Curr Sci 80(1):35–48

Biesboer DD, Mahlberg PG (1978) Accumulation of non-utilizable starch in laticifers of *Euphorbia heterophylla* and *E. myrsinites*. Planta 143(1):5–10

Bilia AR, Santomauro F, Sacco C, Bergonzi MC, Donato R (2014) Essential oil of *Artemisia annua* L.: an extraordinary component with numerous antimicrobial properties. Evid Based Complement Altern Med 2014:7

Booth JK, Page JE, Bohlmann J (2017) Terpene synthases from *Cannabis sativa*. PLoS One 12:e0173911

Briggs WR, Olney MA (2001) Photoreceptors in plant photomorphogenesis to date. Five phytochromes, two cryptochromes, one phototropin, and one superchrome. Plant Physiol 125(1):85–88

Brisibe EA, Umoren UE, Brisibe F, Magalhäes PM, Ferreira JFS, Luthria D, Wu X, Prior RL (2009) Nutritional characterisation and antioxidant capacity of different tissues of *Artemisia annua* L. Food Chem 115(4):1240–1246

Brown GD (2010) The biosynthesis of artemisinin (Qinghaosu) and the phytochemistry of *Artemisia annua* L. (Qinghao). Molecules 15(11):7603–7698

Bryant L, Flatley B, Patole C, Brown GD, Cramer R (2015) Proteomic analysis of *Artemisia annua*—towards elucidating the biosynthetic pathways of the antimalarial pro-drug artemisinin. BMC Plant Biol 15(1):175

Cain AJ (1947) The use of Nile blue in the examination of lipoids. Q J Microsc Sci 88(3):383–392

Coşge Şenkal B, Kiralan M, Yaman C (2015) The effect of different harvest stages on chemical composition and antioxidant capacity of essential oil from *Artemisia annua* L. Tarim Bilim Derg 21:71–77

Demarsy E, Fankhauser C (2009) Higher plants use LOV to perceive blue light. Curr Opin Plant Biol 12(1):69–74

Dutta Gupta S, Karmakar A (2017) Machine vision based evaluation of impact of light emitting diodes (LEDs) on shoot regeneration and the effect of spectral quality on phenolic content and antioxidant capacity in *Swertia chirata*. J Photochem Photobiol B 174:162–172

Ennajdaoui H, Vachon G, Giacalone C, Besse I, Sallaud C, Herzog M, Tissier A (2010) Trichome specific expression of the tobacco (*Nicotiana sylvestris*) cembratrien-ol synthase genes is controlled by both activating and repressing *cis*-regions. Plant Mol Biol 73(6):673–685

Falcioni R, Moriwaki T, Bonato CM, de Souza LA, Nanni MR, Antunes WC (2017) Distinct growth light and gibberellin regimes alter leaf anatomy and reveal their influence on leaf optical properties. Environ Exp Bot 140:86–95

Fan X-X, Xu Z-G, Liu X-Y, Tang C-M, Wang L-W, Han X-l (2013) Effects of light intensity on the growth and leaf development of young tomato plants grown under a combination of red and blue light. Sci Hortic 153:50–55

Fiutak G, Michalczyk M, Filipczak-Fiutak M, Fiedor L, Surówka K (2019) The impact of LED lighting on the yield, morphological structure and some bioactive components in alfalfa (*Medicago sativa* L.) sprouts. Food Chem 285:53–58

Folta K, Carvalho S (2015) Photoreceptors and control of horticultural plant traits. HortScience 50:1274–1280

Folta KM, Pontin MA, Karlin-Neumann G, Bottini R, Spalding EP (2003) Genomic and physiological studies of early cryptochrome 1 action demonstrate roles for auxin and gibberellin in the control of hypocotyl growth by blue light. Plant J 36(2):203–214

Fukuda N, Fujita M, Ohta Y, Sase S, Nishimura S, Ezura H (2008) Directional blue light irradiation triggers epidermal cell elongation of abaxial side resulting in inhibition of leaf epinasty in geranium under red light condition. Sci Hortic 115:176–182

Furr M, Mahlberg PG (1981) Histochemical analyses of latic-ifers and glandular trichomes in *Cannabis sativa*. J Nat Prod 44(2):153–159

Galvão VC, Fankhauser C (2015) Sensing the light environment in plants: photoreceptors and early signaling steps. Curr Opin Neurobiol 34:46–53

Ghasemzadeh A, Ghasemzadeh N (2011) Flavonoids and phenolic acids: role and biochemical activity in plants and human. J Med Plant Res 5(31):6697–6703

Goins GD, Yorio NC, Sanwo MM, Brown CS (1997) Photomorphogen-esis, photosynthesis, and seed yield of wheat plants grown under red light-emitting diodes (LEDs) with and without supplemental blue lighting. J Exp Bot 48:1407–1413

Gonçalves B, Correia CM, Silva AP, Bacelar EA, Santos A, Moutinho-Pereira JM (2008) Leaf structure and function of sweet cherry tree (*Prunus avium* L.) cultivars with open and dense canopies. Sci Hortic 116(4):381–387

Gregory M, Baas P (1989) A survey of mucilage cells in vegetative organs of the dicotyledons. Isr J Bot 38(2–3):125–174

Han J, Wang H, Lundgren A, Brodelius PE (2014) Effects of overex-pression of AaWRKY1 on artemisinin biosynthesis in transgenic *Artemisia annua* plants. Phytochemistry 102:89–96

Hayes S, Velanis CN, Jenkins GI, Franklin KA (2014) UV-B detected by the UVR8 photoreceptor antagonizes auxin sign-aling and plant shade avoidance. Proc Natl Acad Sci USA 111(32):11894–11899

He Q, Fu X, Shi P, Liu M, Shen Q, Tang K (2017) Glandular trichome-specific expression of alcohol dehydrogenase 1 (ADH1) using a promoter-GUS fusion in *Artemisia annua* L. Plant Cell Tissue Organ Cult 130(1):61–72

Ho WE, Peh HY, Chan TK, Wong WSF (2014) Artemisinins: phar-macological actions beyond anti-malarial. Pharmacol Ther 142(1):126–139

Hong G-J, Hu W-L, Li J-X, Chen X-Y, Wang L-J (2009) Increased accumulation of artemisinin and anthocyanins in *Artemisia annua* expressing the arabidopsis blue light receptor CRY1. Plant Mol Biol Rep 27(3):334–341

Inthima P, Nakano M, Otani M et al (2017) Overexpression of the gibberellin 20-oxidase gene from *Torenia fournieri* resulted in

modified trichome formation and terpenoid metabolites of *Arte-misia annua* L. Plant Cell Tissue Organ Cult 129:223–236

Izzo LG, Arena C, De Micco V, Capozzi F, Aronne G (2019) Light quality shapes morpho-functional traits and pigment content of green and red leaf cultivars of *Atriplex hortensis*. Sci Hortic (Amsterdam) 246:942–950

Johansen DA (1940) Plant microtechnique. McGraw-Hill Book Com-pany Inc., New York, p 523

Johkan M, Shoji K, Goto F, Hahida S, Yoshihara T (2012) Effect of green light wavelength and intensity on photomorphogenesis and photosynthesis in *Lactuca sativa*. Environ Exp Bot 75:128–133

Jolliffe HG, Gerogiorgis DI (2016) Plantwide design and economic evaluation of two continuous pharmaceutical manufacturing (CPM) cases: ibuprofen and artemisinin. Comput Chem Eng 91:269–288

Joulian D, König WA (1998) The atlas of spectral data of sesquiterpene hydrocarbons. Pergamon Press, Hamburg, p 658

Judd R, Bagley MC, Li M et al (2019) Artemisinin biosynthesis in non-glandular trichome cells of *Artemisia annua*. Mol Plant 12:704–714

Karimi E, Jaafar HZE, Ghasemzadeh A, Ibrahim MH (2013) Light intensity effects on production and antioxidant activity of fla-vonoids and phenolic compounds in leaves, stems and roots of three varieties of *Labisia pumila* Benth. Aust J Crop Sci 7(7):1016–1023

Kayser O (2018) Ethnobotany and medicinal plant biotechnology: from tradition to modern aspects of drug development. Planta Med 84(12/13):834–838

Kazaz B, Webster S, Yadav P (2016) Interventions for an artemisinin-based malaria medicine supply chain. Prod Oper Manag 25(9):1576–1600

Kim WS, Choi WJ, Lee S, Kim WJ, Lee DC, Sohn UD, Shin HS, Kim W (2015) Anti-inflammatory, antioxidant and antimicrobial effects of artemisinin extracts from *Artemisia annua* L. Korean J Physiol Pharmacol 19(1):21–27

Klermund C, Ranftl QL, Diener J, Bastakis E, Richter R, Schwech-heimer C (2016) LLM-Domain B-GATA transcription factors promote stomatal development downstream of light signaling pathways in hypocotyls. Plant Cell 28(3):646–660

Kong S-G, Suzuki T, Tamura K, Mochizuki N, Hara-Nishimura I, Nagatani A (2006) Blue light-induced association of phototropin 2 with the Golgi apparatus. Plant J 45(6):994–1005

Lazzarini LES, Bertolucci SKV, Pacheco FV, dos Santos J, Silva ST, de Carvalho AA, Pinto JEBP (2018) Quality and intensity of light affect *Lippia gracilis* Schauer plant growth and volatile com-pounds in vitro. Plant Cell Tissue Organ Cult 135(3):367–379

Li H, Xu Z, Tang C (2010) Effect of light-emitting diodes on growth and morphogenesis of upland cotton (*Gossypium hirsutum* L.) plantlets in vitro. Plant Cell Tissue Organ Cult 103(2):155–163

Linstrom PJ, Mallard WG (2016) NIST Chemistry WebBook, NIST Standard Reference Database Number 69. https://doi.org/10.18434/T4D303. Accessed May 2017

Liu C-Z, Zhou H-Y, Zhao Y (2007) An effective method for fast deter-mination of artemisinin in *Artemisia annua* L. by high perfor-mance liquid chromatography with evaporative light scattering detection. Anal Chim Acta 581(2):298–302

Liu M, Xu Z, Guo S, Tang C, Liu X, Jao X (2014) Evaluation of leaf morphology, structure and biochemical substance of bal-loon flower (*Platycodon grandiflorum* (Jacq.) A. DC.) plantlets in vitro under different light spectra. Sci Hortic 174:112–118

Liu M, Shi P, Fu X, Brodelius PE, Shen Q, Jiang W, He Q, Tang K (2016) Characterization of a trichome-specific promoter of the aldehyde dehydrogenase 1 (ALDH1) gene in *Artemisia annua*. Plant Cell Tissue Organ Cult 126(3):469–480

Liu H, Fu Y, Hu D, Yu J, Liu H (2018) Effect of green, yellow and purple radiation on biomass, photosynthesis, morphology and

soluble sugar content of leafy lettuce via spectral wavebands "knock out". Sci Hortic (Amsterdam) 236:10–17

Lommen WJM, Schenk E, Bouwmeester HJ, Verstappen FWA (2006) Trichome dynamics and artemisinin accumulation during development and senescence of *Artemisia annua* leaves. Planta Med 72(04):336–345

Ma D-M, Wang Z, Wang L, Alejos-Gonzales F, Sun M-A, Xie D-Y (2015) A genome-wide scenario of terpene pathways in self-pollinated *Artemisia annua*. Mol Plant 8(11):1580–1598

Ma YN, Chen CJ, Li QQ, Xu FR, Cheng YX, Dong X (2019) Monitoring antifungal agents of *Artemisia annua* against *Fusarium oxysporum* and *Fusarium solani*, associated with *Panax notoginseng* root-rot disease. Molecules 24(1):213

Macedo AF, Leal-Costa MV, Tavares ES, Lage CLS, Esquibel MA (2011) The effect of light quality on leaf production and development of in vitro-cultured plants of *Alternanthera brasiliana* Kuntze. Environ Exp Bot 70(1):43–50

Maes L, Van Nieuwerburgh FCW, Zhang Y, Reed DW, Pollier J, Vande Casteele SRF, Inzé D, Covello PS, Deforce DLD, Goossens A (2011) Dissection of the phytohormonal regulation of trichome formation and biosynthesis of the antimalarial compound artemisinin in *Artemisia annua* plants. New Phytol 189(1):176–189

Maffei M, Scannerini S (1999) Photomorphogenic and chemical responses to blue light in *Mentha piperita*. J Essent Oil Res 11(6):730–738

Mahmoud SS, Croteau RB (2002) Strategies for transgenic manipulation of monoterpene biosynthesis in plants. Trends Plant Sci 7:366–373

Massa GD, Kim H-H, Wheeler RM, Mitchell CA (2008) Plant productivity in response to LED lighting. HortScience 43(7):1951–1956

Mat Daud Z, Awang Y, Ismail F, Mohamed MTM (2016) Effects of red and blue spectrum of light emitting diodes (LEDs) on the growth and photosynthesis of lemon basil (*Ocimum × citriodorum*). III Int Conf Agric Food Eng 1152:183–188

McLafferty FW (2009) Wiley registry of mass spectral data. Wiley, New York

Melillo de Magalhães P, Dupont I, Hendrickx A, Joly A, Raas T, Dessy S, Sergent T, Schneider Y-J (2012) Anti-inflammatory effect and modulation of cytochrome P450 activities by *Artemisia annua* tea infusions in human intestinal Caco-2 cells. Food Chem 134(2):864–871

Mesa LE, Lutgen P, Velez ID, Segura AM, Sara M (2015) *Artemisia annua* L., potential source of molecules with pharmacological activity in human diseases. Am J Phytomed Clin Ther 3:436–450

Milhous WK, Weina PJ (2010) The botanical solution for malaria. Science 327(5963):279–280

Mishra S, Khurana JP (2017) Emerging roles and new paradigms in signaling mechanisms of plant cryptochromes. Crit Rev Plant Sci 36:89–115

Murashige T, Skoog F (1962) A revised medium for rapid growth and bio assays with tobacco tissue cultures. Physiol Plant 15(3):473–497

Nguyen KT, Arsenault PR, Weathers PJ (2011) Trichomes + roots + ROS = artemisinin: regulating artemisinin biosynthesis in *Artemisia annua* L. Vitro Cell Dev Plant 47(3):329–338

O'Brien TP, Feder N, McCully ME (1964) Polychromatic staining of plant cell walls by toluidine blue O. Protoplasma 59(2):368–373

Omer E (2013) Effect of soil type and seasonal variation on growth, yield, essential oil and artemisinin content of *Artemisia annua* L. Int Res J Hortic 1:15

Pacheco FV, de Paula Avelar R, Alvarenga ICA, Bertolucci SKV, de Alvarenga AA, Pinto JEBP (2016) Essential oil of monkey-pepper (*Piper aduncum* L.) cultivated under different light environments. Ind Crops Prod 85:251–257

Paerse A (1980) Seeds of plenty, seeds of want: social and economic implications of the green revolution. Oxford University Press, Oxford, p 262

Pashkovskiy PP, Kartashov AV, Zlobin IE, Pogosyan SI, Kuznetsov VV (2016) Blue light alters miR167 expression and microRNA-targeted auxin response factor genes in *Arabidopsis thaliana* plants. Plant Physiol Biochem 104:146–154

Peplow M (2018) Looking for cheaper routes to malaria medicines. Chem Eng News 96(11):29–31

Perazzo FF, Carvalho JCT, Carvalho JE, Rehder VLG (2003) Central properties of the essential oil and the crude ethanol extract from aerial parts of *Artemisia annua* L. Pharmacol Res 48(5):497–502

Peterson CA, Peterson RL, Robards AW (1978) A correlated histochemical and ultrastructural study of the epidermis and hypodermis of onion roots. Protoplasma 96(1):1–21

Pfaffl MW (2001) A new mathematical model for relative quantification in real-time RT-PCR. Nucleic Acids Res 29(9):e45

Pizzolato TD, Larson PR (1977) Axillary bud development in *Populus deltoides*. II. Late ontogeny and vascularization. Am J Bot 64(7):849–860

Poudel PR, Kataoka I, Mochioka R (2008) Effect of red- and blue-light-emitting diodes on growth and morphogenesis of grapes. Plant Cell Tissue Organ Cult 92(2):147–153

Pu G-B, Ma D-M, Wang H, Ye H-C, Liu B-Y (2013) Expression and localization of amorpha-4,11-diene synthase in *Artemisia annua* L. Plant Mol Biol Rep 31(1):32–37

Reale S, Fasciani P, Pace L, Angelis FD, Marcozzi G (2011) Volatile fingerprints of artemisinin-rich *Artemisia annua* cultivars by headspace solid-phase microextraction gas chromatography/mass spectrometry. Rapid Commun Mass Spectrom 25(17):2511–2516

Ren J, Guo S, Xu C, Yang C, Ai W, Tang Y, Qin L (2014) Effects of different carbon dioxide and LED lighting levels on the antioxidative capabilities of *Gynura bicolor* DC. Adv Space Res 53(2):353–361

Ruan J-X, Li J-X, Fang X, Wang L-J, Hu W-L, Chen X-Y, Yang C-Q (2016) Isolation and characterization of three new monoterpene synthases from *Artemisia annua*. Front Plant Sci 7:638. https://doi.org/10.3389/fpls.2016.00638

Schuerger AC, Brown CS, Stryjewski EC (1997) Anatomical features of pepper plants (*Capsicum annuum* L.) Grown under red light-emitting diodes supplemented with blue or far-red light. Ann Bot 79:273–282

Shi P, Fu X, Liu M, Shen Q, Jiang W, Li L, Sun X, Tang K (2017) Promotion of artemisinin content in *Artemisia annua* by overexpression of multiple artemisinin biosynthetic pathway genes. Plant Cell Tissue Organ Cult 129(2):251–259

Singh D, Basu C, Meinhardt-Wollweber M, Roth B (2015) LEDs for energy efficient greenhouse lighting. Renew Sustain Energy Rev 49:139–147

Su N, Wu Q, Shen Z, Xia K, Cui J (2013) Effects of light quality on the chloroplastic ultrastructure and photosynthetic characteristics of cucumber seedlings. Plant Growth Regul 73:227–235

Sultana S, Hu H, Gao L, Mao J, Luo J, Jongsma MA, Wang C (2015) Molecular cloning and characterization of the trichome specific chrysanthemyl diphosphate/chrysanthemol synthase promoter from *Tanacetum cinerariifolium*. Sci Hortic 185:193–199

Tan H, Xiao L, Gao S, Li Q, Chen J, Xiao Y, Ji Q, Chen R, Chen W, Zhang L (2015) TRICHOME AND ARTEMISININ REGULATOR 1 is required for trichome development and artemisinin biosynthesis in *Artemisia annua*. Mol Plant 8(9):1396–1411

Tariq U, Ali M, Abbasi BH (2014) Morphogenic and biochemical variations under different spectral lights in callus cultures of *Artemisia absinthium* L. J Photochem Photobiol B 130:264–271

Tzenkova R, Kamenarska Z, Draganov A, Atanassov A (2010) Composition of *Artemisia annua* essential oil obtained from

species growing wild in Bulgaria. Biotechnol Biotechnol Equip 24(2):1833–1835

Untergasser A, Nijveen H, Rao X, Bisseling T, Geurts R, Leunissen JA (2007) Primer3Plus, an enhanced web interface to Primer3. Nucleic Acids Res 35(Web Server issue):W71–W74

van Den Dool H, Kratz PD (1963) A generalization of the retention index system including linear temperature programmed gas—liquid partition chromatography. J Chromatogr A 11:463–471

Wang Y, Zhang H, Zhao B, Yuan X (2001) Improved growth of *Artemisia annua* L hairy roots and artemisinin production under red light conditions. Biotechnol Lett 23(23):1971–1973

Wang E, Gan S, Wagner GJ (2002) Isolation and characterization of the CYP71D16 trichome-specific promoter from *Nicotiana tabacum* L. J Exp Bot 53(376):1891–1897

Wang H, Liu Y, Chong K, Liu BY, Ye HC, Li ZQ, Yan F, Li GF (2007) Earlier flowering induced by over-expression of CO gene does not accompany increase of artemisinin biosynthesis in *Artemisia annua*. Plant Biol 9(3):442–446

Wang H, Han J, Kanagarajan S, Lundgren A, Brodelius PE (2013) Trichome-specific expression of the amorpha-4,11-diene 12-hydroxylase (cyp71av1) gene, encoding a key enzyme of artemisinin biosynthesis in *Artemisia annua*, as reported by a promoter-GUS fusion. Plant Mol Biol 81(1):119–138

World Health Organization (2016) Artemisinin and artemisinin-based combination therapy resistance: status report, vol WHO/HTM/GMP/2016.5. World Health Organization, Geneva, p 12

World Health Organization (2017) World Malaria Report 2017. World Health Organization, Geneva, p 161

Wu H, Guo J, Chen S, Liu X, Zhou Y, Zhang X, Xu X (2013) Recent developments in qualitative and quantitative analysis of phytochemical constituents and their metabolites using liquid chromatography–mass spectrometry. J Pharm Biomed 72:267–291

Wu Q, Su N, Shen W, Cui J (2014) Analyzing photosynthetic activity and growth of *Solanum lycopersicum* seedlings exposed to different light qualities. Acta Physiol Plant 36:1411–1420

Xiao L, Tan H, Zhang L (2016) *Artemisia annua* glandular secretory trichomes: the biofactory of antimalarial agent artemisinin. Sci Bull 61(1):26–36

Xie D-Y, Ma D-M, Judd R, Jones AL (2016) Artemisinin biosynthesis in *Artemisia annua* and metabolic engineering: questions, challenges, and perspectives. Phytochem Rev 15(6):1093–1114

Xu W, Zou Z, Pei J, Huang L (2018) Longitudinal trend of global artemisinin research in chemistry subject areas (1983–2017). Bioorg Med Chem 26:5379–5387

Yadav RK, Sangwan RS, Sabir F, Srivastava AK, Sangwan NS (2014) Effect of prolonged water stress on specialized secondary metabolites, peltate glandular trichomes, and pathway gene expression in *Artemisia annua* L. Plant Physiol Biochem 74:70–83

Yu W, Liu Y, Song L, Jacobs DF, Du X, Ying Y, Shao Q, Wu J (2017) Effect of differential light quality on morphology, photosynthesis, and antioxidant enzyme activity in *Camptotheca acuminata* seedlings. J Plant Growth Regul 36(1):148–160

Zhang D, Sun W, Shi Y, Wu L, Zhang T, Xiang L (2018) Red and blue light promote the accumulation of artemisinin in *Artemisia annua* L. Molecules 23(6):1329

Zhao S, Fernald RD (2005) Comprehensive algorithm for quantitative real-time polymerase chain reaction. J Comput Biol 12(8):1047–1064

Zheng L, Van Labeke MC (2017) Long-term effects of red-and blue-light emitting diodes on leaf anatomy and photosynthetic efficiency of three ornamental pot plants. Front Plant Sci 8:917

Zhigzhitzhapova SV, Dylenova EP, Gulyaev SM, Randalova TE, Taraskin VV, Tykheev ZA, Radnaeva LD (2019) Composition and antioxidant activity of the essential oil of *Artemisia annua* L. Nat Prod Res. https://doi.org/10.1080/14786419.2018.1548461

Affiliations

Ellen M. Lopes[1] · Fábia Guimarães-Dias[2] · Thália do S. S. Gama[3] · Arthur L. Macedo[4,9] · Alessandra L. Valverde[4] · Marcela C. de Moraes[5] · Ana Cristina A. de Aguiar-Dias[6] · Humberto R. Bizzo[7] · Marcio Alves-Ferreira[2] · Eliana S. Tavares[8] · Andrea F. Macedo[1]

[1] Integrated Laboratory of Plant Biology (LIBV), Institute of Biosciences, Department of Botany, Federal University of Rio de Janeiro State (UNIRIO), Avenida Pasteur nº 458, 5th Floor, Room 512, Rio de Janeiro, RJ CEP: 22290-240, Brazil

[2] Laboratory of Plant Molecular Genetics (LGMV), Institute of Biology, Department of Genetics, Federal University of Rio de Janeiro (UFRJ), Rio de Janeiro, RJ, Brazil

[3] Laboratory of Plant Anatomy (LAV), Institute of Biosciences, Department of Botany, University of São Paulo (USP), São Paulo, SP, Brazil

[4] Laboratory of Natural Products (LaProMar), Institute of Chemistry, Fluminense Federal University (UFF), Niterói, RJ, Brazil

[5] Laboratory of Chromatography and Screening Strategies, Institute of Chemistry, Fluminense Federal University (UFF), Niterói, RJ, Brazil

[6] Laboratory of Plant Anatomy (LAV), Institute of Biosciences, Department of Botany, Federal University of Rio de Janeiro State (UNIRIO), Rio de Janeiro, RJ, Brazil

[7] Brazilian Agricultural Research Corporation (Embrapa), Food Agroindustry, Rio de Janeiro, RJ, Brazil

[8] Laboratory of Plant Anatomy, Institute of Biology, Department of Botany, Federal University of Rio de Janeiro (UFRJ), Rio de Janeiro, RJ, Brazil

[9] Present Address: Post-Graduate Program in Pharmacy, Laboratory of Natural Products and Mass Spectrometry (LaPNEM), Faculty of Pharmaceutical Sciences, Food and Nutrition, Federal University of Mato Grosso do Sul (UFMS), Campo Grande, MS, Brazil